Nuclear Engineering and Design 304 (2016) 125–138

Contents lists available at ScienceDirect

Nuclear Engineering and Design

journal homepage: www.elsevier.com/locate/nucengdes

Probabilistic seismic safety assessment of a CANDU 6 nuclear power plant including ambient vibration tests: Case study

Ali Nour [a,b,*], Abdelhalim Cherfaoui [a], Vladimir Gocevski [a], Pierre Léger [b]

[a] Hydro Québec, Montréal, Québec H2L4P5, Canada
[b] École Polytechnique de Montréal, Montréal, Québec H3C3A7, Canada

HIGHLIGHTS

- In this case study, the seismic PSA methodology adopted for a CANDU 6 is presented.
- Ambient vibrations testing to calibrate a 3D FEM and to reduce uncertainties is performed.
- Procedure for the development of FRS for the RB considering wave incoherency effect is proposed.
- Seismic fragility analysis for the RB is presented.

ARTICLE INFO

Article history:
Received 19 January 2016
Received in revised form 2 May 2016
Accepted 5 May 2016
Available online 27 May 2016

JEL classification:
L. Safety and Risk Analysis

ABSTRACT

Following the 2011 Fukushima Daiichi nuclear accident in Japan there is a worldwide interest in reducing uncertainties in seismic safety assessment of existing nuclear power plant (NPP). Within the scope of a Canadian refurbishment project of a CANDU 6 (NPP) put in service in 1983, structures and equipment must sustain a new seismic demand characterised by the uniform hazard spectrum (UHS) obtained from a site specific study defined for a return period of 1/10,000 years. This UHS exhibits larger spectral ordinates in the high-frequency range than those used in design. To reduce modeling uncertainties as part of a seismic probabilistic safety assessment (PSA), Hydro-Québec developed a procedure using ambient vibrations testing to calibrate a detailed 3D finite element model (FEM) of the containment and reactor building (RB). This calibrated FE model is then used for generating floor response spectra (FRS) based on ground motion time histories compatible with the UHS. Seismic fragility analyses of the reactor building (RB) and structural components are also performed in the context of a case study. Because the RB is founded on a large circular raft, it is possible to consider the effect of the seismic wave incoherency to filter out the high-frequency content, mainly above 10 Hz, using the incoherency transfer function (ITF) method. This allows reducing significantly the non-necessary conservatism in resulting FRS, an important issue for an existing NPP. The proposed case study, and related methodology using ambient vibration testing, is particularly useful to engineers involved in seismic re-evaluation of existing NPP.

1. Introduction

Within the scope of the refurbishment project of a 675 MW CANDU 6 PHWR (Pressurized Heavy Water Reactor) NPP built from 1973–1983, structures and equipment should sustain a new seismic demand characterized by a UHS obtained from a site specific study and defined for a return period of 1/10,000 years (Hydro Quebec, 2009a). Compared to the original seismic design demand based on Newmark–Housner type of response spectrum, the UHS for the site exhibits larger spectral ordinates in the high frequency range than the original design spectrum.

Regulatory standard S-294 (2005) requires implementing PSA for both internal and external events. Following the 2011 Fukushima Daiichi nuclear accident in Japan, there is a worldwide interest in reducing uncertainties in seismic safety assessment of existing NPP. The current research emphasis is on developing robust methodology to re-evaluate the flood and seismic hazard and risk within the context of PSA (Ake et al., 2015; Mandal et al., 2016; Muta et al., 2016). Mandal et al. (2016) report post Fukushima Daiichi research on seismic fragility analysis of Indian PHWR in operation since 1973. Different approaches are compared to compute the seismic fragility curves including incremental dynamic analysis (IDA) with detailed nonlinear FE model using displacement based failure limit states. It is mentioned that the conventional method

* Corresponding author at: Hydro Québec, Montréal, Québec H2L4P5, Canada.

http://dx.doi.org/10.1016/j.nucengdes.2016.05.004
0029-5493/

based on the peak ground acceleration (PGA) to construct fragility curves do not capture aleatory (randomness) uncertainty properly.

In order to meet the regulatory standard S-294 (2005), Hydro Quebec first conducted a state-of-the-art site specific seismic hazard study (Hydro-Québec, 2009a). Then an ambient vibration method was used to calibrate a detailed 3D FEM of the containment wall (CW) structure and reactor building (RB) internal structure (IS) and reduce aleatory and epistemic uncertainties. A simplified method to consider seismic wave incoherency effect at high frequency on the raft foundation was also introduced (EPRI, 2006). Different records of ground motion time histories compatible with UHS were used to compute FRS and to conduct classical seismic fragility for structures (EPRI, 1994, Kennedy et al., 1980). This paper presents this procedure in the context of a case study of the RB and demonstrates its benefits in reducing uncertainties in PSA for an existing NPP.

For this NPP, the use of classical techniques for generating FRS leads to very high peaks in the high-frequency range for seismic excitations in the range of 10 Hz and above. These peaks may cause difficulties in assessing or qualifying equipment sensitive to this range of frequencies. The CANDU 6 reactor building considered herein is founded on a very large raft foundation. EPRI reports (2005, 2006, 2007) indicate that seismic wave incoherency filter out the high-frequency content of input motions. Seismic compression and shear waves propagating from the hypocenter to the mat foundation encounter multiple reflections and refractions resulting in spatially incoherent variations as they encounter rock mass discontinuities. Moreover, as seismic waves reach the nearly rigid concrete foundation mat there is also an averaging effect of incoherent motions as they propagate to the supported reactor IS. This results in a significant reduction in FRS peaks, leading to a more realistic determination of the seismic demands for RB equipment.

In this paper, the calibrated 3D FEM for the RB is used for generating FRS based on ground motion time histories compatible with the median UHS for assessing existing equipment through fragility analyses described in the EPRI document (1994), and time histories compatible with the mean UHS for performing design of new equipment. Furthermore, the seismic wave incoherency effect is considered to reduce the ground motion intensity and filter out the high frequency content, mainly from 10 Hz and above. The incoherency transfer function (ITF) method proposed by EPRI (2006) is implemented herein into the commercial finite element code Ds-Simulia ABAQUS (2008). This allows reducing significantly the non-necessary conservatism in resulting FRS which is an important issue for an existing NPP.

For this NPP, PSA allows safety evaluation considering on a rational basis the aleatory and epistemic uncertainties within the scope of the regulator requirements. In PSA, seismic fragility analysis is an important step in the evaluation of the seismic margin with regard to the capacity of components (structures) of the plant to sustain the new seismic demand. The resulting performance index from the seismic fragility analysis is the High Confidence of Low Probability of Failure (HCLPF) seismic capacity, defined in terms of the selected seismic parameter.

This case study presents the methodology adopted for the seismic fragility analyses of a CANDU 6 reactor building (Hydro-Quebec, 2010b). The fragility analyses are mainly based on EPRI (1991; 1994; 2002) documents combined with structural models calibrated with ambient vibrations measurements results to reduce epistemic uncertainties. The results are presented for the CW and for the IS of the reactor.

The industrial application of this seismic PSA was performed in a context where three imperatives must be properly balanced. First, the technical soundness and acceptance by regulatory agencies is of primary importance in selecting the details of an appropriate seismic PSA methodology. It must be recognized that there is always a significant delay before research developments are transformed in a format suitable for industrial applications and subsequent acceptance by regulatory agencies. Second, there was a limited time frame to conduct this seismic PSA study to renew the operating license and maintain continuous operations of the NPP. Third, the seismic PSA had to be conducted within predefined budgetary constraints based on the first two imperatives. We strongly believe that this case study is of value to the professional community and illustrates the benefit of using ambient vibration tests in seismic safety assessment of existing NPP. The adopted methodology for this CANDU 6 NPP is particularly useful to engineers involved in the analyses of complex structural systems.

2. Site specific seismic hazard study: UHS, selection and scaling of ground motions

A site specific study, as documented in Hydro-Quebec (2009a), incorporates recent developments on the seismicity of the region where the NPP is located, by considering a paleo-seismological investigation referring to the status of sediments (presence of an earthquake or not reported by liquefaction) and their dating. The paleo-seismological study was done for the Rabaska site, a deep-water terminal capable of accommodating large methane tankers to be located downstream of this NPP along the St-Lawrence river (Tuttle, 2008). Within this framework an updated seismic demand characterized by a UHS is obtained. As shown in Fig. 1, this UHS is defined for a return period of 1/10,000 years and for different confidence level (median and mean). Compared to the original design basis earthquake DBE-1974 (AECL, 1974) based on Newmark-Housner type of ground response spectrum, the UHS for the site exhibits larger spectral ordinates in the high frequency range.

Moreover, Atkinson (Hydro Quebec, 2009b) developed six ground motion time history records to spectrally match the UHS target spectrum for the site, on rock, for the median confidence level. This confidence level is generally selected for the seismic assessment of existing structures and equipment as stated in EPRI (1994) and NEA/CSNI-9 (2015) documents. Three median records (two horizontal and a vertical component for each ground motion) are obtained from seismological simulations (Set 1: M7 at R = 60 km; Set 2: M7 at R = 60 km; Set 3: M7 at R = 60 km) where M is the moment magnitude and R is the hypocentral distance from the site.

Three other records are obtained from spectral matching technique by modifying the frequency content of historical recorded ground motions (i) BB: BroadBand, M7.3 R42 km, Landers, CA 1994; (ii) LF: Low Frequency, M > 7 R60 to 70 km, Chi-Chi, Taiwan

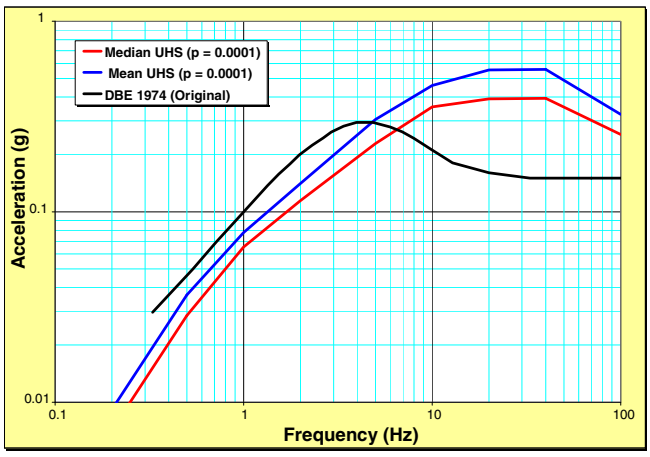

Fig. 1. Updated seismic demand (UHS) for the site.

1999; (iii) HF: High Frequency, M6 R20 km, Saguenay 1988. The seismic records Sets 1–3 are considered separately, and the BB signal is considered as an additional record. The combination of LF (Set 5) and HF (Set 6) signals constitutes complementary records to cover adequately the frequency range of the target site specific UHS. A BB ground motion record was also developed to match the target spectrum for the CANDU 6 NPP site (1/10,000 p.a.), on rock, for the mean confidence level (Hydro-Québec, 2009b). This record is obtained from spectral matching technique by modifying the frequency content of historical recorded ground motions (M7.3 R42 km, 1994 Landers earthquake, CA, USA).

All signals presented in Figs. 2 and 3 meet the ASCE 4-98 (2000) and 43-05 (2005) as well as the CSA-N289.3 (2010) requirements for earthquake records to be used in seismic safety assessment of existing NPP facilities (i.e. criteria regarding duration, time interval, spectrum compatibility, power spectral density and stochastic independence). Figs. 2 and 3 show these signals that are matching the target response spectrum in both, horizontal and vertical directions. The UHS target spectrum was developed initially for the horizontal motion component. The corresponding vertical spectrum for rock sites is defined following Atkinson (Hydro-Québec, 2009b), based on the frequency-dependent V/H ratios published for rock sites in Eastern North America (ENA). This V/H ratio = 1 at low frequencies, decreasing to slightly more than 2/3 at high frequencies ($\geqslant$10 Hz).

Here, the mean confidence level is selected to perform new refurbishment design works in agreement with CSA N289.2 (2010) and NEA/CSNI-9 (2015) documents. According to Adams (2015), the median values represents the 50th% percentile of the distribution (approx. 1 chance out of two to be exceeded) while the mean is at 65th% to 75th% of the distribution (approx. 1 chance out of 3 to be exceeded). In comparison to conventional buildings where the seismic requirements in the NBCC (2010) for design are based on the median confidence level, a higher confidence level (mean) is used for nuclear buildings to increase the public confidence in the safety of nuclear power plants. Note that the mean

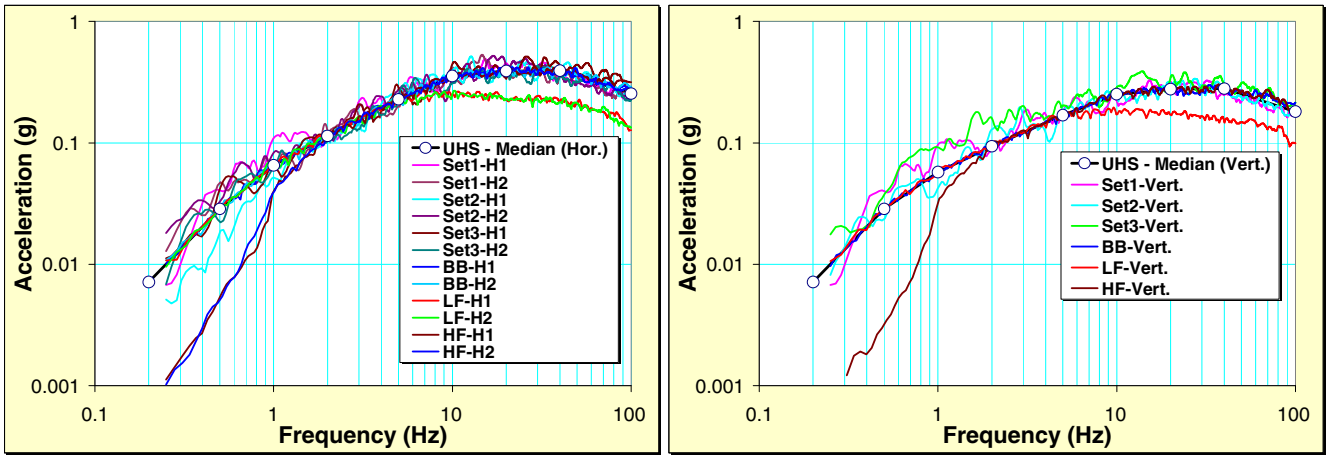

a. Response spectra.

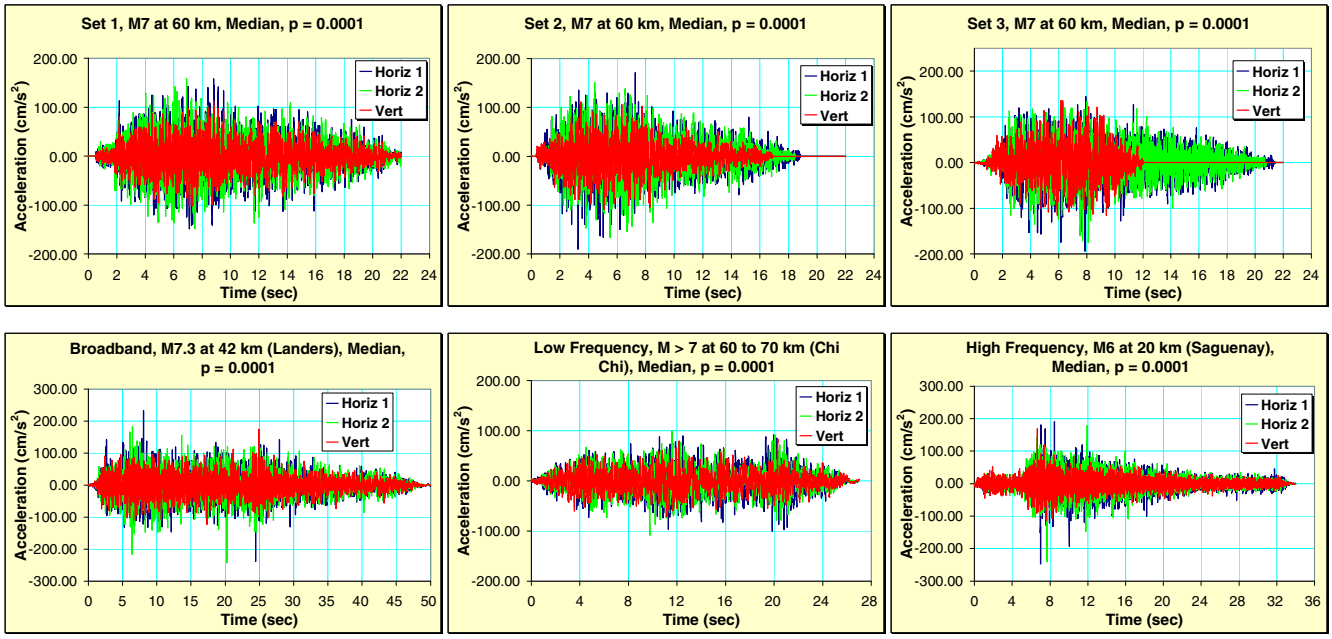

b. Time histories.

Fig. 2. Ground motion time histories compatibles with the median UHS.

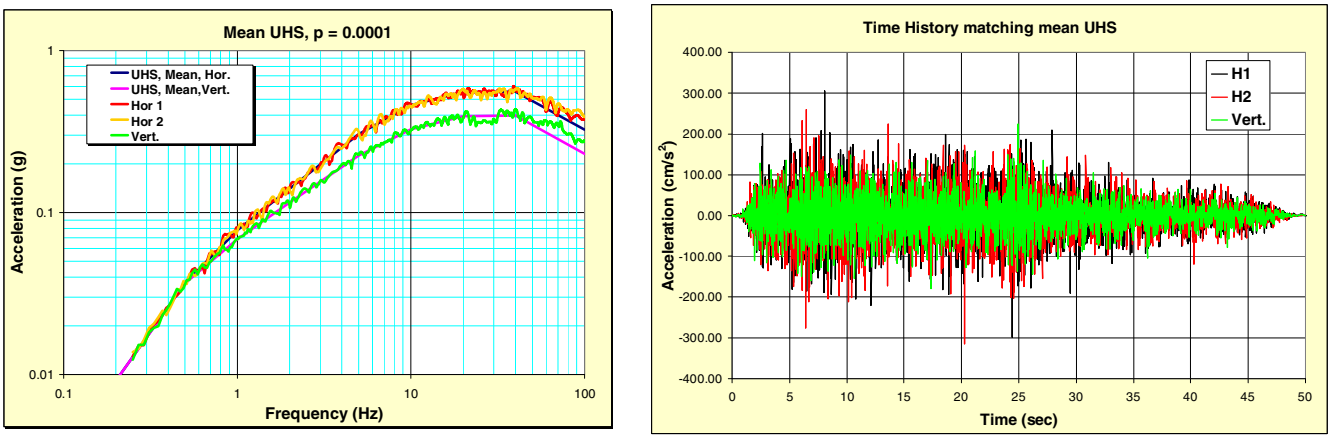

a. Response spectra. b. Time histories.

Fig. 3. Ground motion time histories compatibles with the mean UHS for the site of study.

hazard values are introduced in NBCC (2015) (Adams, 2015). McGuire et al. (2005) pointed out that "no single measure of seismic hazard (e.g., a mean or median estimate)" is adequate to represent the lack of understanding in seismic hazard estimates and related uncertainties. They recommended that mean estimate should be used when a single estimate is necessary instead of the median or a particular fractile level of seismic hazard. They argue that the mean better reflects all important sources of aleatory and epistemic uncertainties when a single number is required. On the other hand, Abrahamson and Bommer (2005) argue that the mean hazard curve "blurs the distinction between aleatory variability and epistemic uncertainties". They recommended that a particular fractile may be considered appropriate such as the 85th fractile or even the median if deemed appropriate.

In this study, mean values are used to design anchorage for new equipment using a single BB record that envelopes the target spectrum (mean UHS) via deterministic calculation, while median seismic excitations were used to explicitly introduce aleatory and epistemic uncertainties to compute the 95th fractile corresponding to the High-Confidence-Low-Probability-of-Failure (HCLPF) capacity computed from the fragility curve of concern for the failure mechanism under scrutiny.

3. Safety goals and acceptance criteria for the CANDU 6 NPP

To demonstrate the safety of the plant against severe accident, it is required that the result of the PSA of the CANDU 6 meet some safety goals. These safety goals are based on internationally established criteria for existing plants (IAEA INSAG-12, 1999) and are in accordance with the safety goals proposed by the Canadian Nuclear Safety Commission (CNSC) in regulatory document RD-152 (2009). In this context, one should demonstrate that the contribution of seismic events to Severe Core Damage Failure (SCDF) and Large Release Failure (LRF) is low and the plant meets its safety goals. As stated in the NUREG-1407 (1991) document, the safety goal for the LRF is an order of magnitude lower than that of the SCDF. However, the adopted safety goals for this plant corresponding to SCDF and LRF are 1.0E-4/yr and 3.0E-5/yr, respectively (Hydro-Quebec, 2010a). The seismic-induced SCDF/LRF is typically obtained from seismic PSA by integrating the seismic hazard, seismic capacity of the structure (or component), and the plant response. Herein, the structural capacity is characterized by the HCLPF. The shape of the UHS adopted as the reference for this seismic PSA is quite different from that of the initial DBE spectrum. Thus the PGA may not be appropriate for using as a reference frequency for HCLPF. Damage is heavily influenced by the duration and the frequency content of the ground motion versus the predominant frequency of the structure. Thus the spectral acceleration in the range of about 2–8 Hz is more significant to characterize the damage potential of ground motions than PGA (EPRI, 1991). On this basis, the frequency having average spectral acceleration between 5 Hz and 10 Hz is considered as the reference frequency for presenting the HCLPF (Hydro-Quebec, 2010a). The average spectral acceleration between 5 and 10 Hz is estimated to be 7.4 Hz. Fig. 4 shows mean occurrence frequency versus spectral acceleration at 7.4 Hz derived from the seismic hazard assessment of the site of study. The seismic fragility analysis is based on the median UHS, and calculated HCLPF capacity of the structure (component) equivalent to 7.4 Hz is compared with the acceptance criteria (SCDF and LRF) based on the mean UHS, i.e. on criteria relatively higher than the median UHS. In fact, the spectral acceleration of 1.0E-4/yr return frequency is 0.38 g and that of the 3.0E-5/yr return frequency is 0.8 g. Therefore, this plant should meet the following acceptance criteria:

- The plant HCLPF capacity for severe core damage should be larger than 0.38 g spectral acceleration at 7.4 Hz.

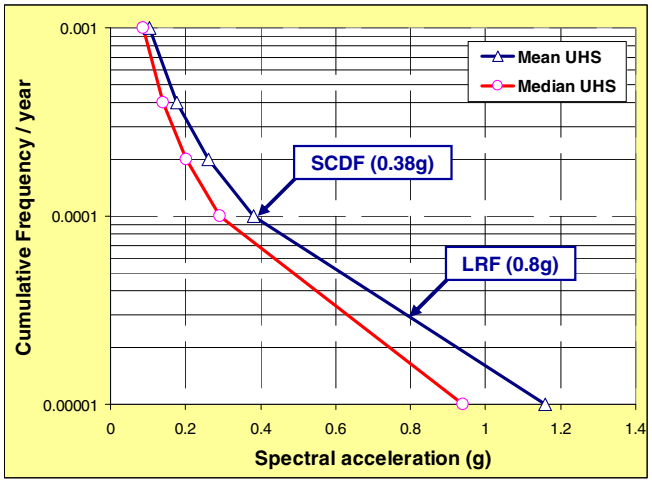

Fig. 4. Seismic Hazard curves for the CANDU 6 at 7.4 Hz spectral acceleration.

- The plant HCLPF capacity for large release should be larger than 0.8 g spectral acceleration at 7.4 Hz.

4. Finite element model and seismic analyses for the CANDU 6 reactor building

The CANDU 6 reactor building has the function of lodging the reactor, auxiliary equipment, machinery and the necessary facilities for handling fuel. It consists of two distinct parts, the CW and the IS (Fig. 5). The CW is a prestressed concrete structure composed of a circular raft foundation, with a thickness of 1.5 m and a diameter of 47 m. It contains also a cylindrical wall, with a thickness of 1.05 m and an inner radius of 20.7 m as well as a spherical dome with a central thickness of 0.61 m with a radius of 41.5 m. Just below this dome there is a second reinforced concrete spherical dome having an opening in the center. This element serves as a water reservoir for emergency shutdown with a capacity of about 2540 m^3. The IS is mainly a reinforced concrete structure, designed to support the reactor vessel and the various pieces of equipment.

4.1. Tridimensional finite element model for the CANDU 6 reactor building

The 3D FEM of the reactor building includes the IS and the CW sharing the same foundation raft (Fig. 5). The concrete raft is founded on stiff rock rigid boundary conditions at the rock-concrete interface. It was developed using the FE software ABAQUS (2008). A detailed 3D FEM, if developed adequately and controlled for convergence (e.g. the missing mass effect is corrected by static correction), is more accurate and less conservative than a traditional beam-column stick model with lumped masses for seismic analysis of NPP (Varpasuo, 1999). The 3D FEM is preferred to the stick model as the equipment requalification for an existing structure, depends directly on the FRS. Because at this stage one is basically interested in the displacement field and its derivatives with respect to time (velocity and acceleration), 10 node quadratic tetrahedral isoparametric solid elements with a linear strain representation (C3D10) are used for the model (Fig. 5).

One major advantage of this element is fast automatic meshing, with regards to the complexity of the reactor building structure. Furthermore, the quadratic C3D10 solid element is more accurate than the linear 4 node tetrahedral solid element (C3D4).

The updated seismic demand has significantly increased as compared to the initial design requirements. To develop an unbiased seismic assessment of the reactor building (existing structure), one has to work to reduce to the extent feasible the uncertainties of the key parameters controlling the seismic behavior. Hence, the weight of the heavy equipment and their locations were assigned with special care. This issue required an exhaustive review of drawings as well as equipment catalogs (CANATOM, 1973).

The equipment masses are introduced in the model in two ways, (i) non-structural masses for the calandria vault system, the dousing water system and the live load for the different floors, and (ii) lumped concentrated masses for important equipment. The concrete calandria shell is part of the FEM and fluid–structure interaction is not considered in this study. Therefore, the dousing water and the calandria fluid are modeled as non-structural masses. The elastic properties used for the dynamic analyses, after

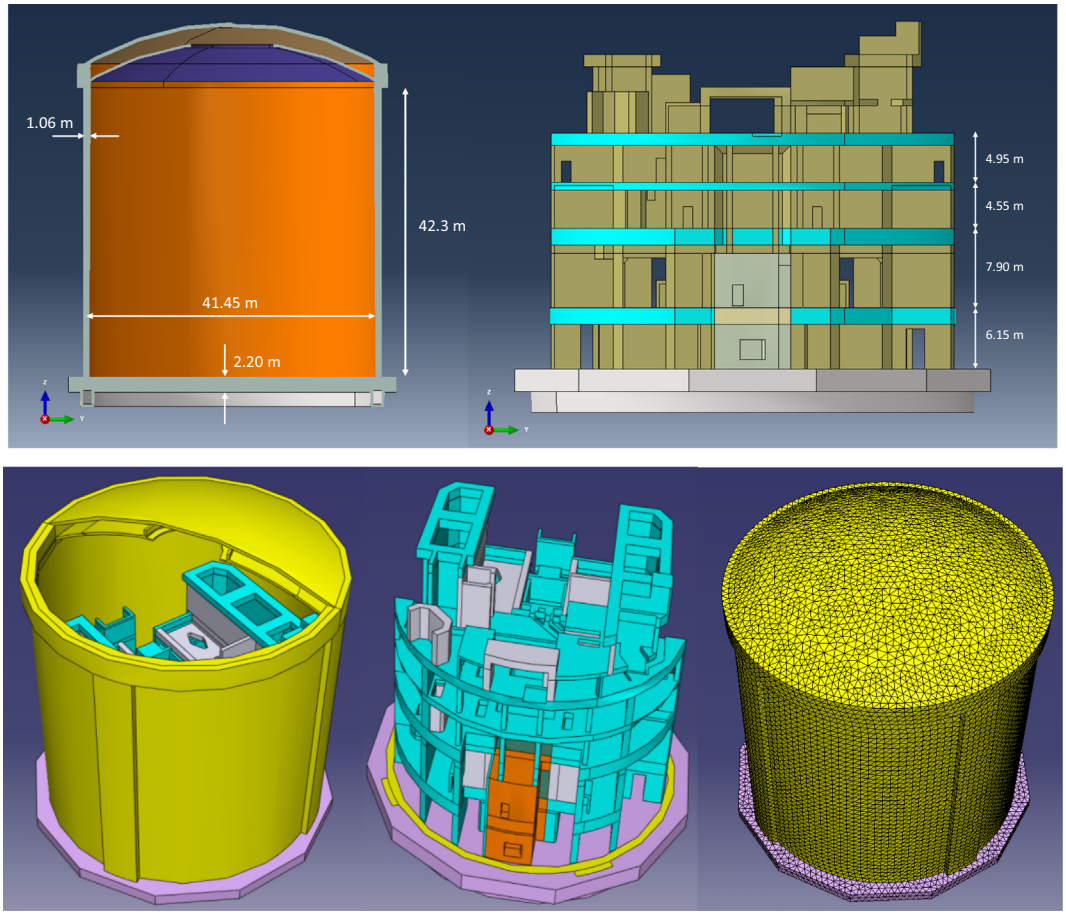

Fig. 5. CANDU 6 reactor building and 3D FE model.

Table 1
Elastic properties for the reinforced/prestressed concrete.

	Elastic modulus (MPa)	Poisson ratio	Density (kg/m^3)
IS heavy concrete	28,500	0.18	3650
IS regular concrete	28,500	0.18	2500
CW concrete	30,000	0.18	2500

Table 2
Summary of testing data.

	Internal structure (IS)	Containment wall (CW)
Frequency of acquisition	200 Hz	200 Hz
Duration of the acquisition	300 s	300 s
Total number of measurement	10	8

calibration of the numerical model with the ambient vibration measurement, are as follow (see Table 1):

The initial design properties are based on concrete compression strength of 5000 psi (≈35 MPa) for the CW and 4000 psi (≈27 MPa) for the IS.

4.2. Seismic analyses of the CANDU 6 reactor building

Linear seismic analyses are performed using the modal transient dynamic procedure with modal composite damping which allows assigning fractions of the critical damping for different materials, such that an equivalent modal damping is computed from modal strain energy equivalence. Hence, for the dynamic analysis, a composite modal damping, considering 3% for the prestressed concrete structure and 5% for the reinforced concrete structure is used. Because all equipment has small masses compared to the mass of the structure, equipment-structure interaction is neglected. Thus, only the masses of the equipment (without stiffness) are considered in the numerical model. The Lanczos technique is used for the solution of the eigenvalue problem and all modes ⩽100 Hz are considered. Therefore, the missing mass corresponding to modes above 100 Hz is captured through the static correction technique by introducing a residual mode in the modal analysis.

4.3. Ambient vibration measurement and calibration of the finite element model (FEM)

To account for the actual dynamic properties of the structure, the numerical model is first calibrated by adjusting the effective stiffness of structural components with ambient vibrations measurements. Then, the different load conditions are introduced in the model. Only few NPPs around the world were tested for ambient vibrations (Choi et al. 2010). Choi et al. (2013) reported the ambient vibration test of 4 containment structures in South Korea including the Wolsung 2 CANDU 6 unit (678 MW) in operation since 1997, however no results were reported for the internal structures. To the best of the author's knowledge we are presenting the first ambient test results for the internal structure of a CANDU 6 reactor building. The ambient vibration testing program was performed for some selected buildings of the CANDU 6 NPP including the reactor building (internal and the envelope structures). The scope of these measurements is to determine the actual dynamic properties (fundamental frequencies and mode shapes) to be used for calibrating the numerical models and to ensure that the inertia and the stiffness of the numerical model correspond to the real structure.

The ambient vibration measurements have been performed using the Granite data acquisition system manufactured by the company Kinemetrics (2007). This system consists of a high performance portable twelve channel data acquisition system with a maximum sampling frequency of 2000 Hz. To get maximum sensitivity for each sensor, the internal jumpers were set to obtain a maximum acceleration range of ±0.25 g using a ±20 volts differential excitation. Table 2 provides summary of testing data.

The data processing has been performed by IZIIS (2008) using the ARTEMIS software. After filtering the time history records, both techniques of Frequency Domain Decomposition (FDD) and Enhanced FDD (EFDD) are used to determine dominant frequencies and the relative mode shapes for the IS and CW. The coherency function and the random decrement techniques are used to distinguish between the structural versus the operational modes (machinery vibration). These analyses were validated, in the framework of Hydro-Québec quality-insurance, through independent analyses by Lamarche (2008) using MATLAB in-house subroutines. Hence, from the numerical model, the first natural frequencies are computed and compared to results obtained from ambient vibration testing. Fig. 6 shows the first natural frequencies obtained from the calibrated numerical model (IS and CW) as well as their corresponding mode shapes.

Recently, the Wolsung Unit 2 (similar to the CANDU under study) was instrumented for ambient vibration measurements and a frequency of 8.09 Hz was identified for the first mode of the CW (Choi et al., 2013). For this CANDU (Wolsung Unit 2), Choi et al. (2008) provided results of the free vibration analyses of the CW based on the nominal elastic values, and the first frequency is around 3.8 Hz. It is not obvious to understand the difference between the actual frequency from tests (8.09 Hz) and the one obtained from design data (3.8 Hz). For our case, the first frequency for the CW obtained from the ambient vibration measurements is around 4.2 Hz. This value is in accordance with the results reported by Choi et al. (2008).

4.4. Fixed base model justification

According to AECL (1974), the reactor building is built on a rock site where the shear wave velocity Vs varies from 1500 m/s to 2200 m/s, thus the free field deconvolution and the soil structure interaction are neglected. Therefore, a fixed base mathematical model is adopted as explained below:

- In the NS-G-3.6 safety guide of the IAEA (2004), it is mentioned that for type 1 sites (Vs > 1100 m/s), a fixed base could be adopted for the numerical model.
- In Section 3.3.3.2 of the ASCE 4-98 (2000), it is well indicated that the bottom rigid boundary of the numerical model could be defined at the soil layer having Vs > 1100 m/s. Because the shear wave velocity of the underlying soil layer of the site under study is greater than 1500 m/s, this rigid boundary coincides with the foundation base of the reactor building. Furthermore, as shown in Fig. 7, Section 3.3.1.1 of ASCE 4-98 (2000) requirements are satisfied, then a fixed base is adopted for the numerical model.

5. Procedure for the development of FRS for the CANDU 6 reactor building considering wave incoherency effect

In this study a clear distinction is made between (1) the seismic safety assessment of *existing* component and equipment following EPRI (1994) fragility computational framework, discussed in Section 6.1, and (2) the design of *new* equipment as per applicable regulatory standards CSA N289.2-(2010) and NEA/CSNI-9 (2015). The advantage of this dual approach is to use high confidence safety

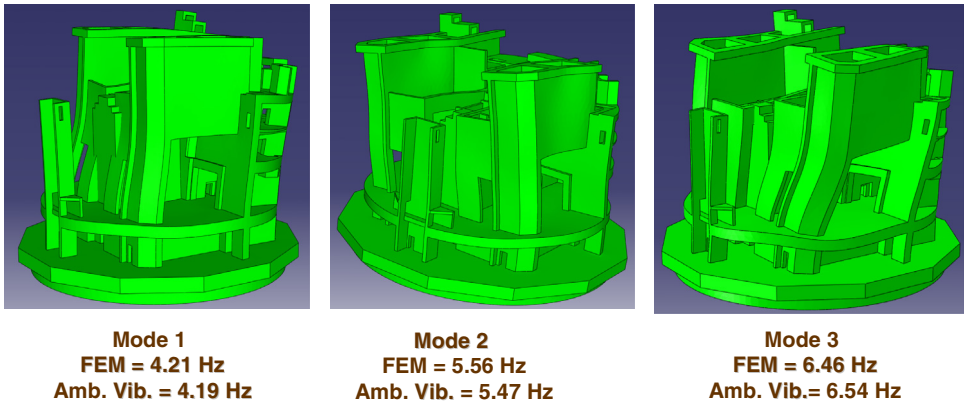

a. Internal structure.

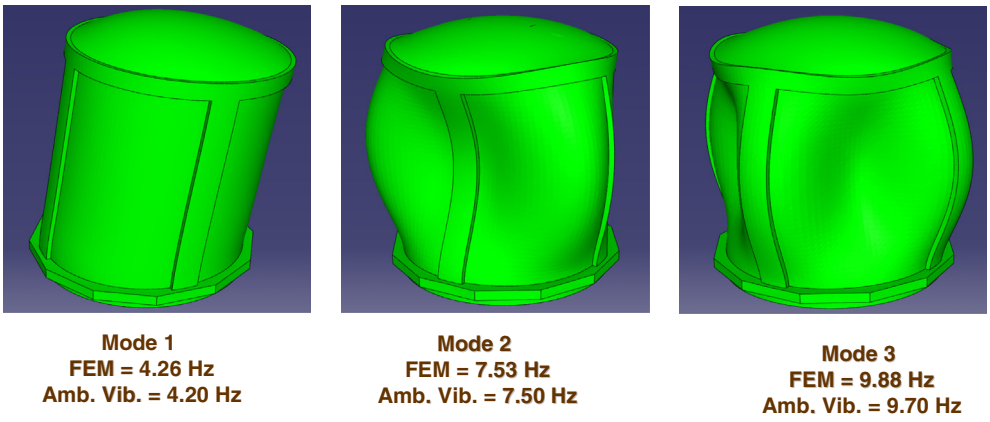

b. Containment wall.

Fig. 6. Calibration of the finite element model (FEM) with ambient vibrations (Amb. Vib.) results.

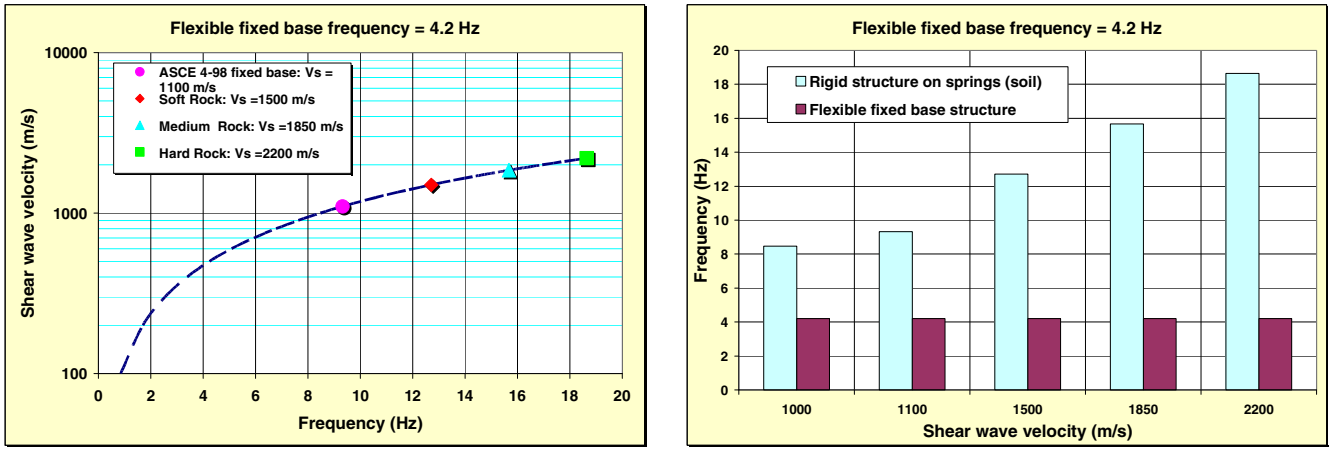

a b

Fig. 7. Fixed base model justification (mode 1 ≅ 4.2 Hz in Fig. 6).

level for new designs reflected by relatively higher seismic requirements compared to those adopted for existing equipment. It was therefore decided to use the median UHS as a reference spectrum for the seismic assessment in the framework of the seismic PSA methodology to evaluate existing equipment. The design changes that will be performed during the refurbishment outage and the life extension are based on the mean UHS as input requirements using a single BB record.

For the development of the reactor building FRS, one first performs a transient modal seismic analysis by computing the structural response history in the time domain. Then, for the desired point, and for a predefined viscous damping ratio of the

equipment, FRS are computed from the transient accelerations. As recommended by ASCE 4-98 (2000) and CSA-N289.3 (2010), the frequency content of the generated FRS should be broadened to ±15% to account for structural uncertainties. Moreover, a 15% in peak spectral amplitude is considered reasonable to represent a probability of non-exceedance not less than 90% for the seismic assessment of subsystem (ASCE 4-98, 2000).

5.1. FRS for the seismic assessment of equipment in the framework of the seismic PSA methodology

Time histories compatible with the median UHS are used to generate FRS for assessing existing equipment through fragility analyses described in the EPRI document (1994). Because one is developing FRS for an existing NPP, then, one should adopt earthquakes scenarios affecting the equipment using what is perceived as the most representative seismic demand accounting for epistemic as well as aleatory uncertainties. A recommended approach is for the equipment assessment is to use the mean of the computed responses as permitted by ASCE/SEI 43-05 (5 records). Hence, according to ASCE/SEI 43-05 (Section 3.3.2):

- at least 3 records of compatible accelerograms shall be used (simulated; modified historical),
- if less than 5 accelerograms are used, then the largest response (envelope) shall be used,
- if 5 or more accelerograms are used, then the mean of the calculated responses may be used,

From the 3D FEM, the FRS could be generated by adopting one of the following options:

- Option "a": Envelope of FRS calculated from Set 1, Set 2 and Set 3.
- Option "b": Envelope of FRS calculated from BB, LF and HF.
- Option "c": Because LF and HF are considered as complementary events, we first produce the envelope of LF and HF {Lf-Hf = max. (LF, HF)}. Then, we calculate the mean value of the responses from the five (5) groups of results, i.e., Set 1, Set 2, Set 3, BB and Lf-Hf. Thus, the ASCE/SEI 43-05 recommendations are met.

This procedure is described for a single floor, i.e. for the 80'-9" level corresponding to the NS component. Fig. 8a shows the response spectra after peak reduction and broadening the frequency content by ±15% for the six seismic records Set 1, Set 2, Set 3, BB, LF and HF. In Fig. 8b, the non-broadened FRS for the five records, Set 1, Set 2, Set 3, BB and Lf-Hf are plotted by considering a

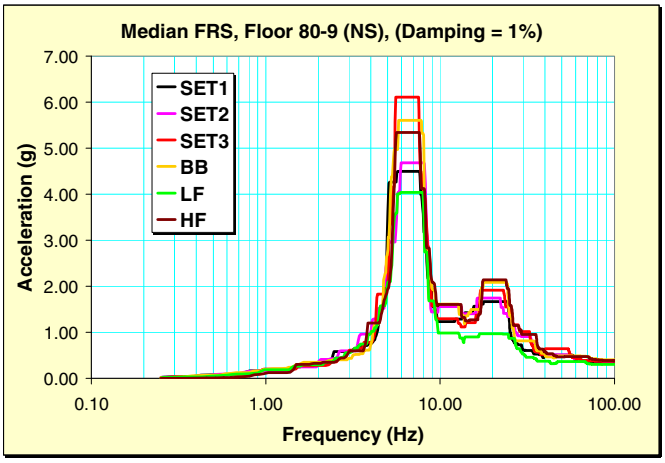

a

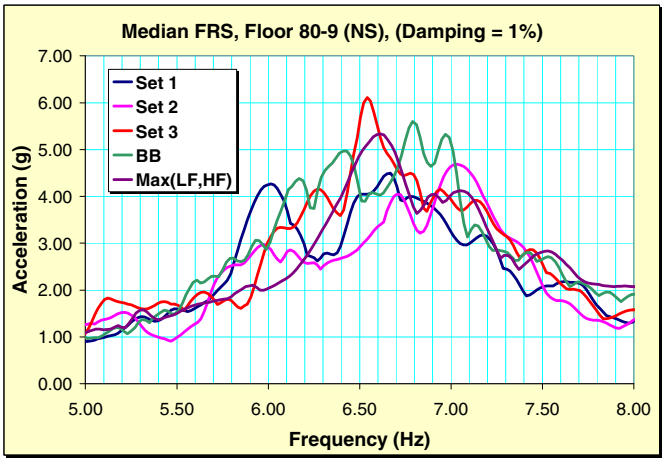

b

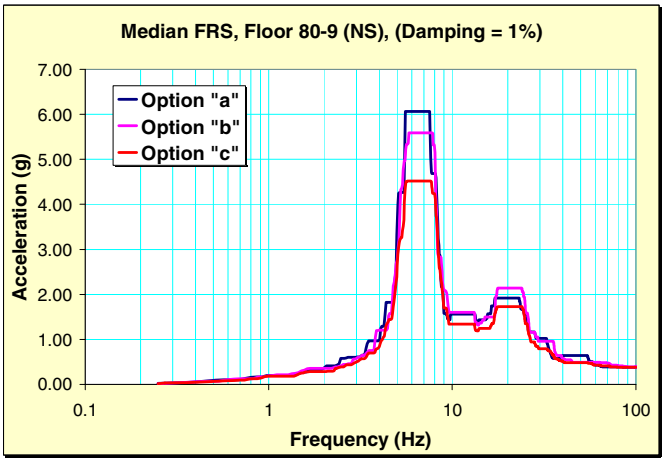

c

Fig. 8. FRS calculations according to options "a", "b" and "c".

zoom near the dominant frequency of the floor. The peak FRS for each record is not obtained exactly at the same frequency, which is due to stochastic nature of seismic records. This is advantageous for an existing structure for which a mean of several seismic records is considered in the generation of the seismic requirements (FRS) for the requalification of equipment.

Fig. 8c depicts the FRS obtained from the three options "a", "b" and "c". Here, the broadening of the frequency content is realized after the computation of the envelope of Max (Set 1, Set 2, Set 3), and of Max (BB, LF, HF) for the options "a" and "b" respectively, and after the calculation of the mean of Set 1, Set 2, Set 3, BB and max (LF, HF) corresponding to the option "c".

The generation of the seismic (FRS) meeting prescribed guideline requirements for an existing building may be conservative if the option "a" or "b" is adopted, or if one deals with only one seismic record that matches the target spectrum (ex: the BB record).

For the equipment assessment using time histories compatible with the median UHS, the option "c" was adopted as it is found to be an adequate and representative approach for this CANDU 6 NPP refurbishment project. Following option "c", the FRS for the IS and the CW were computed at different elevations and for different damping ratios corresponding to the three directions "EW", "NS" and "Vert". In this paper, we present typical results, as shown in Fig. 9, only the FRS at the elevation 80′–9″ corresponding to 1%, 3%, 5%, 7% and 10% of critical damping ratios.

For this FRS based on the median UHS, the seismic wave incoherency effect could be considered to reduce the ground motion intensity and filter out the high frequency content, mainly from 10 Hz and above, as explained in the next section.

5.2. FRS for the seismic design work

For performing new design, FRS based only one BB record of ground motion time histories compatible with the mean UHS is used. Moreover, it is possible to take advantage of the beneficial effect of the seismic wave incoherency as the RB is founded on a large raft. In this case, high frequencies are filtered out and peak FRS are significantly reduced. This incoherency can be incorporated into the FEM using the ITF method documented in EPRI (2006), approved by the U.S. NRC and recommended by the Canadian standard for CANDU CSA-N289.1 (2008, see clause B7). This method consists of modifying the seismic motion at the foundation base to account for the ground motion incoherency via a simplified approach. Moreover, this latter can be easily implemented in some commercial software without performing the exhaustive soil-structure interaction procedure available in the SASSI (System for Analysis of Soil Structure Interactions) computer program (EPRI, 2007; El Khoraibi et al., 2014). EPRI (2006) develops an equivalent method (ITF) to the integrated approach in SASSI to consider the seismic wave incoherency. As demonstrated in EPRI (2006), the

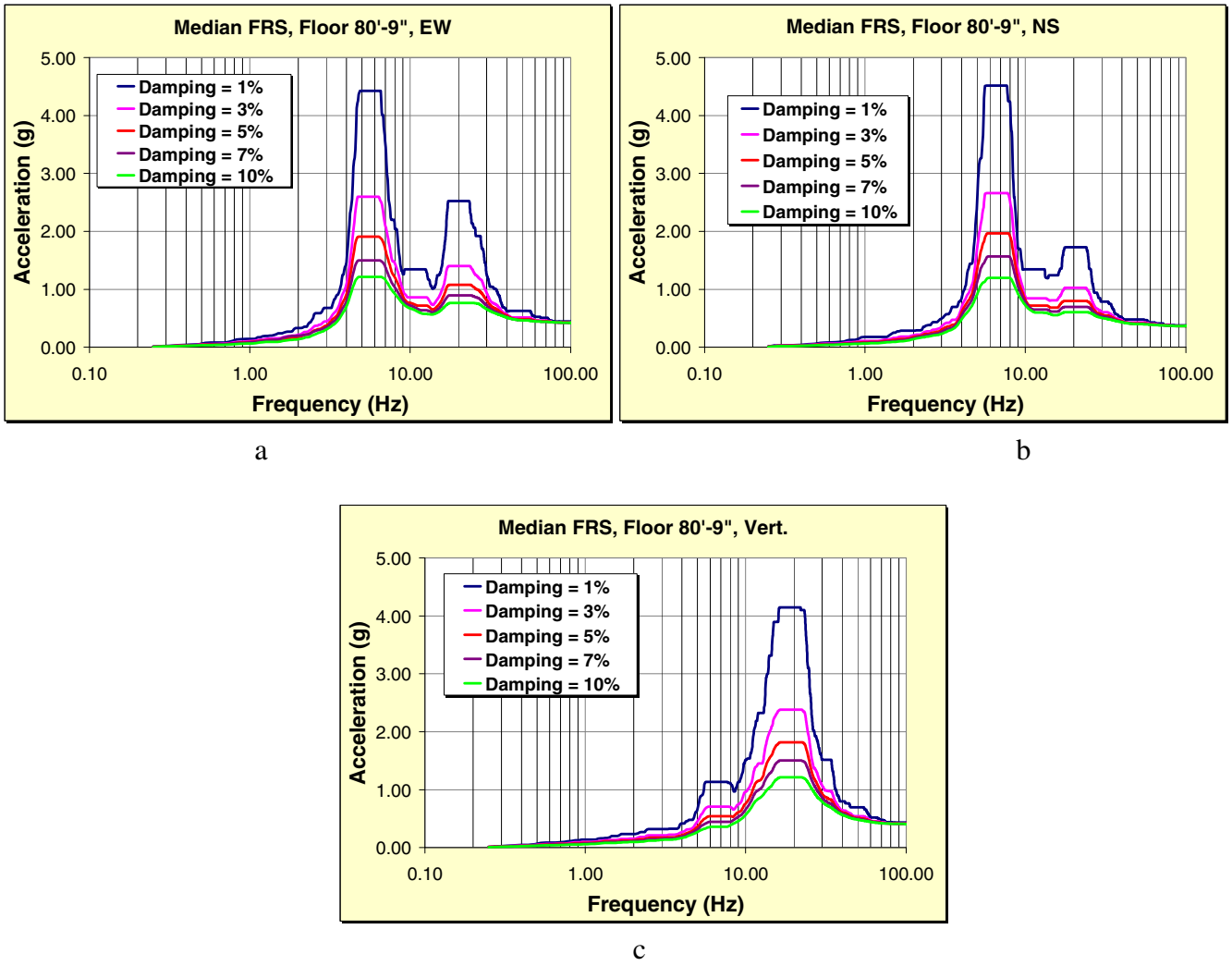

Fig. 9. FRS for the floor 80′–9″ of the internal structure according to options "c".

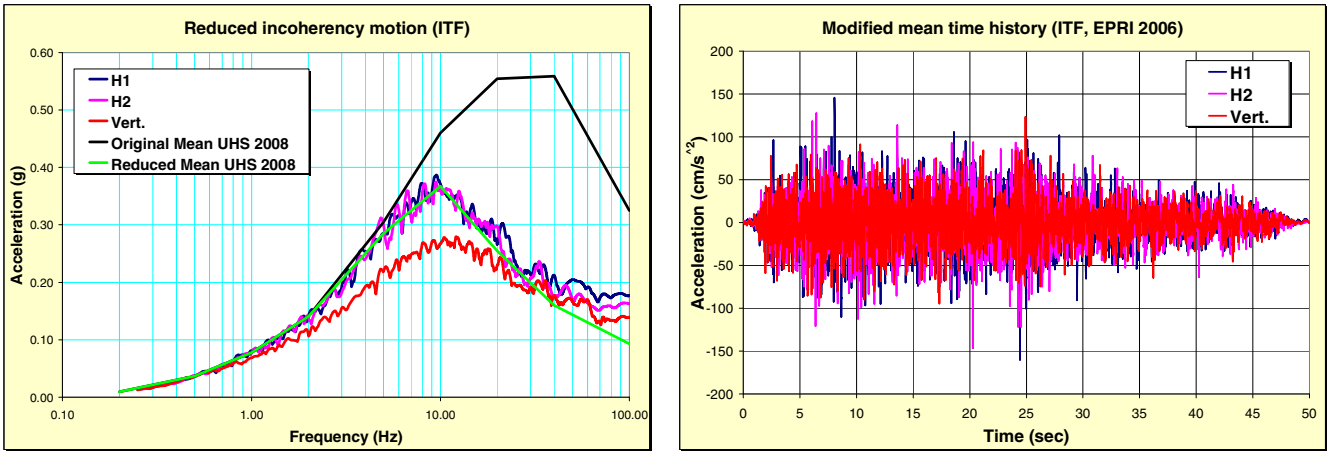

Fig. 10. Reduced incoherency motion using the ITF method.

ITF method gives results slightly conservative but comparable to results obtained from the SASSI program.

The ITF procedure is demonstrated herein for the case of the BB record of ground motion time histories compatible with the mean UHS (Fig. 3b). The same procedure can also be applied for the six ground motion time history records that match the median UHS. Fig. 10a shows the scaling functions based on ITFs in the frequency domain. These scaling functions are applied to modify the amplitude of the Fourier transform coefficients of the free-field ground motions. The modified ground motions (Fig. 10b) are used herein in standard seismic response analyses, using ABAQUS (2008), as an alternate means of including effects of seismic wave incoherency. Different scaling functions are applied for horizontal and vertical motions corresponding to rock site condition. However, it is anticipated that seismic demand will be significantly reduced for high-frequency, mainly from 10 Hz and above.

As shown in Fig. 11, the results of the ITF procedure are described for a single floor, i.e. for the 89′–9″ level and for the three components EW, NS and vertical. Fig. 11a, c and e shows the calculated FRS at this level for different values of damping considering the effect of wave incoherency. Whereas, Fig. 11b, d and f illustrate, for a given damping value of 5%, the results while considering or neglecting the effect of wave incoherency.

In the high-frequency range, it is well demonstrated that the consideration of the beneficial effect of wave incoherency for the reactor building leads to a reduced seismic demand and, therefore, to a realistic design of equipment sensitive to high-frequency content, namely for 10 Hz and above.

6. Seismic fragility analysis of the CANDU 6 NPP reactor building

6.1. Seismic fragility curves

The seismic fragility of a structure can be defined by the conditional probability of failure for a given seismic parameter, i.e., the PGA or the spectral ordinate around the fundamental frequency of the structure. The capacity estimation in terms of the selected seismic parameter is generally obtained from the available information in the design basis. This includes the geometry of the structure, material properties, and the structural response considering the seismic design data. There are several sources of randomness (aleatory) and epistemic uncertainties that affect the accurate estimation of the structural capacity of each potential failure mode. These sources of uncertainty can affect significantly the structural capacity expressed in sustainable acceleration of the structure. Therefore, the seismic fragility is usually described by a family of curves associated with a predefined probability value to reflect the level of confidence in the estimation of the fragility. The fragility A of the structure corresponding to a particular failure mode can be expressed in terms of the median ground acceleration capacity A_M and the two random variables ε_R and ε_U as follows (Kennedy et al., 1980):

$$A = A_M \cdot \varepsilon_R \cdot \varepsilon_U \tag{1}$$

Here, ε_R and ε_U are random variables having median values equal to unity. They represent the inherent randomness around the median value and the epistemic uncertainty in the median capacity value. They are supposed to have a lognormal distribution with logarithmic standard deviations β_R and β_U, respectively. The uncertainty in the evaluation of the fragility is usually expressed in terms of family values of the probability of failure for a given value of ground acceleration (or the chosen seismic intensity parameter). Thus, the probability p that the conditional probability of failure p_f exceeds a specified value p_f', for a given ground acceleration value "a" (the selected seismic parameter), is given by (Kennedy et al., 1980):

$$p\left[\frac{p_f > p_f'}{a}\right] = \phi\left[\frac{\ln\{(\frac{a}{A_M}) \cdot \exp[\beta_R \cdot \phi^{-1}(p_f')]\}}{\beta_U}\right] \tag{2}$$

The conditional probability of failure p_f' for a no-exceedance probability, Q, can be expressed as follows (Kennedy et al., 1980):

$$p_f' = \phi\left[\frac{\ln(\frac{a}{A_M}) + \beta_U \cdot \phi^{-1}(Q)}{\beta_R}\right];\ Q = 1 - P \tag{3}$$

where $\phi(x)$ is the cumulative function of the standard Gaussian distribution; $\phi^{-1}(x)$ denotes the inverse function, Q is the probability of no-exceeding, in practice the values of 5%, 50% and 95% are often used.

6.2. High confidence of low probability of failure (HCLPF) for structures

Following the methodology described in EPRI (1994), and used for the seismic risk assessment for more than 50 NPP in the United States, the high confidence (95%) for a low Probability of Failure (5%) is defined by the following equation:

$$HCLPF = A_M \cdot \exp[-1.65 \cdot (\beta_R + \beta_U)] \tag{4}$$

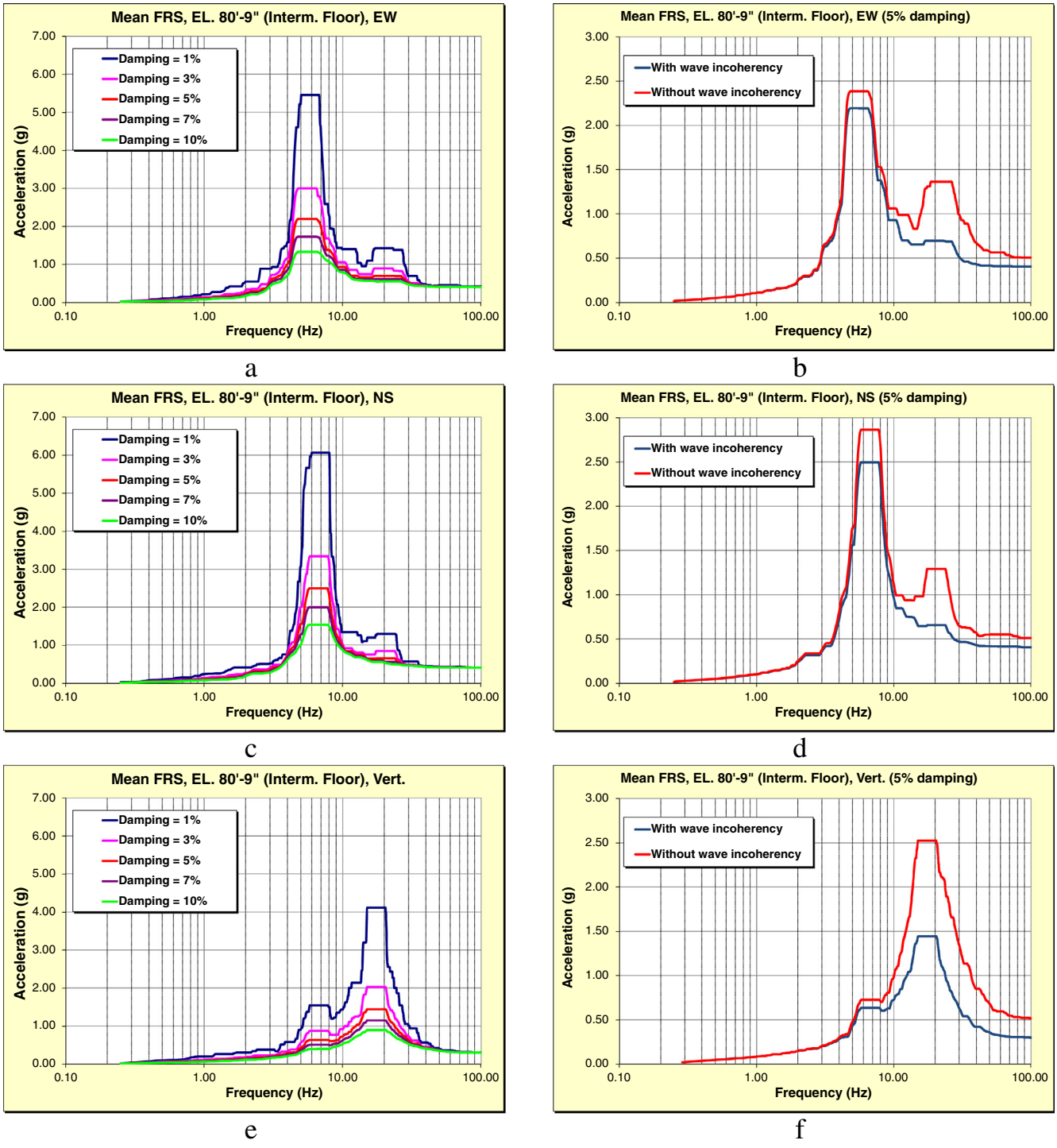

Fig. 11. FRS for the floor 89′–9″ of the internal structure considering wave incoherency effect.

The median ground motion capacity is defined by:

$$A_M = F_M \cdot A_{UHS} \tag{5}$$

where F_M is the median safety factor and A_{UHS} represents the median spectral ordinate of the median UHS (Hydro-Quebec, 2009a). A_{UHS} is determined around the reference period $T_1 = 1/(7.4Hz)$ as recommended by the Seismic Design Guide for this CANDU 6 NPP (Hydro-Quebec, 2009a):

$$A_{UHS} = Sa(T_1) = \frac{1}{(T_1^+ - T_1^-)} \int_{-T}^{+T} Sa(T) \cdot dT \tag{6}$$

To reflect the uncertainty over the reference period, a ±15% variation is considered, i.e., $T_1^- = 0.85 \cdot T_1$ and $T_1^+ = 1.15 \cdot T_1$. It is now clear that the selected seismic intensity parameter for the seismic fragility analysis is A_{UHS}, because as indicated in the EPRI documents (1994, 2002), the use of the PGA introduces additional uncertainties in the analysis. Moreover, the structural frequencies of interest are in most cases below 10 Hz, i.e., too far from the frequency at which the PGA is defined (around 100 Hz in our case). This allows a more accurate seismic risk determination.

The scope of the seismic fragility analysis is to evaluate the seismic margins in the structural response by examining the data used

in the design and their comparison with the current reality of the structure. In other words, it is necessary to eliminate conservatism to find the median seismic capacity. For structures, the global median safety factor F_M is defined as (EPRI, 1994):

$$F_M = F_C \cdot F_{SR} \tag{7}$$

F_C represents the seismic capacity factor and F_{SR} is the structural response factor. F_C is expressed as follows:

$$F_C = F_S \cdot F_\mu \tag{8}$$

F_μ: is the inelastic energy absorption factor. It is determined by estimating the de-amplification of post-elastic structural response due to the ductility combined with the mobilised damping in the facility.

F_S: is the safety factor. It represents the relationship between the ultimate resistance, for which there is loss of functionality of the structural element, and the current resistance.

F_{SR}: is defined as the product of all factors influencing the variability of the structural response, namely: the seismic motion factor, the surface ground motion wave incoherency factor, the factor which accounts for the structural modeling, the factor that accounts for the modal combination of different modes of vibration, the factor that considers the combination of structural responses due to different earthquake components and the soil-structure interaction factor.

The randomness β_R and the uncertainty β_U associated with the median safety factor are defined as follows (EPRI, 2002):

$$\beta_R = \sqrt{\beta_{R\_S}^2 + \beta_{R\_\mu}^2 + \beta_{R\_SR}^2}$$
$$\beta_U = \sqrt{\beta_{U\_S}^2 + \beta_{U\_\mu}^2 + \beta_{U\_SR}^2} \tag{9}$$

where

β_{R_S},β_{U_S}: randomness and uncertainty associated with the strength factor.

β_{R_μ},β_{U_μ}: randomness and uncertainty associated with the inelastic energy absorption factor.

β_{R_SR},β_{U_SR}: randomness and uncertainty associated with the structural response factor.

6.3. Median seismic motions

As recommended by EPRI (1994, 2002), seismic fragility analysis for structures must be conducted using median seismic inputs. The energy dissipation in the structures, to response levels close to the material elastic limit, is assumed generally to depend on the velocity which is similar to the behavior of a viscous damper. In fact, the damping is estimated from the observations and is considered to depend on the strain level. In this context, EPRI (1994) recommends values for material damping depending on the stress state that is half of the elastic limit, near or above the elastic limit. For seismic fragility analyses, the damping values to a stress level close to the elastic limit should be used.

The median UHS was developed for a damping coefficient of 5%. For other damping levels, it is recommended to use the method of Atkinson and Pierre (2004) which is very appropriate for sites in Eastern North America (ENA). In this case, as shown in Fig. 12, the 5% spectrum is modified by coefficients that depend on the frequency (Atkinson and Pierre, 2004).

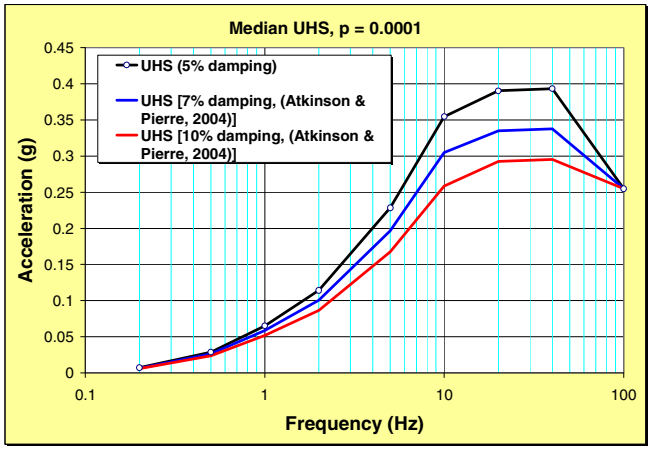

Fig. 12. UHS for different damping values.

6.4. Seismic evaluation of the reactor building capacity

For structures similar to the containment wall, recent studies conducted on the other CANDU NPP (Park et al., 1998; Lee and Song, 1999; Choi et al., 2008) showed that the most critical failure mode corresponds to the tangential shear at the base. It is found

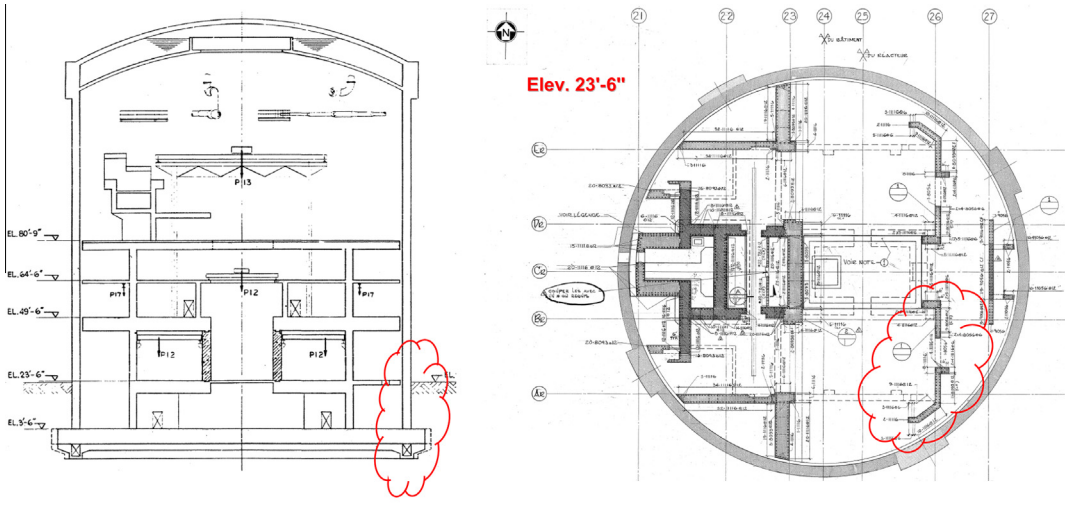

a. Containment wall b. Internal structure

Fig. 13. Critical zones for the reactor building.

that this failure mode is governing as well, for the containment wall of the CANDU 6 reactor building in this case study (see Fig. 13a).

The capacity in terms of HCLPF for this failure mode represents the lowest value among all potential failure modes. The containment wall is locally reinforced by adding steel reinforcements and by increasing the wall thickness at critical penetrations and airlocks. Therefore, the failure in these areas will not govern.

The calculation details of the high confidence of low probability of failure (HCLPF) for the CW are presented in Hydro-Quebec (2010b). However, the synthesis of the results is given in Table 3, and the fragility curves corresponding to 95%, median (50%), mean and 5% confidence levels are shown in Fig. 14a.

For the IS, seismic analyses results showed that the most critical element of this structure is the shear wall located at the axis 26 (see Fig. 13b). This shear wall has an opening of 10 feet (3.05 m) width between the elevations 23′–6″ and 50′–2″. It is found that this part is the most critical for the entire shear wall. Therefore, the seismic fragility analyses of the internal structure are conducted for this shear wall at this location. The capacity in terms of HCLPF for this failure mode represents the lowest value among all potential failure modes.

Table 3
HCLPF for the CW and the IS.

			β_R		β_U	
	CW	IS	CW	IS	CW	IS
Strength factor (F_S)	11.73	4.35	0	0	0.25	0.21
Inelastic energy absorption factor (F_μ)	2.02	2.09	0.09	0.08	0.26	0.26
Structural response factor (F_{SR})	1.16	1.35	0.22	0.24	0.21	0.22
Global safety factor (F_M)	27.37	12.32	0.24	0.26	0.42	0.40
Median capacity in acceleration ($A_M(g)$)	CW			IS		
	8.00			3.60		
HCLPF (*g*)	CW			IS		
	2.73			1.22		

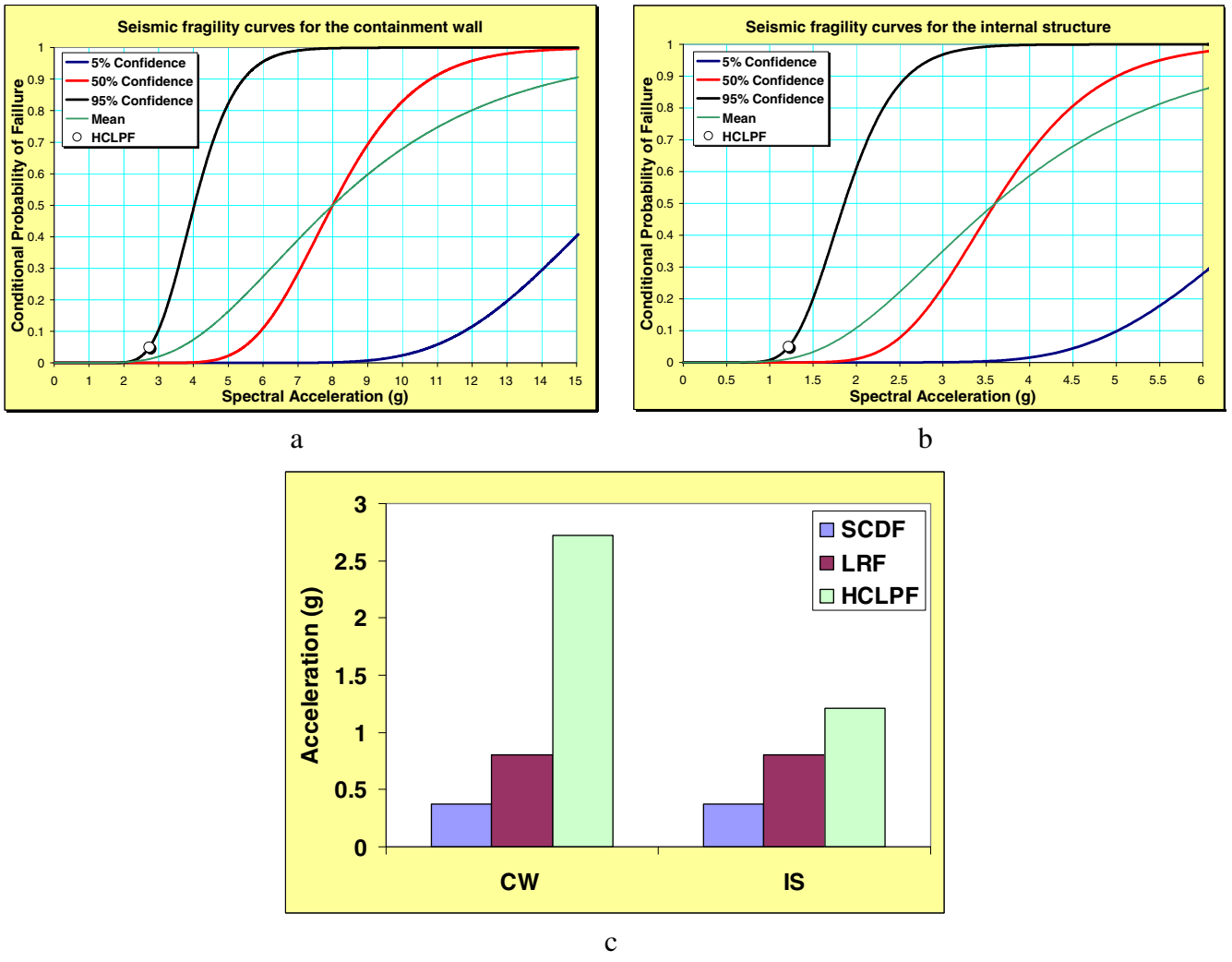

Fig. 14. Seismic fragility curves for the CW and the IS.

The calculation details of the high confidence of low probability of failure (HCLPF) for the IS are presented in Hydro-Quebec (2010b). However, the synthesis of the results is given in Table 3, and the fragility curves corresponding to 95%, median (50%), mean and 5% confidence levels are shown in Fig. 14b.

The computed global safety factors are large (Table 3). This demonstrates that the original design was very robust (large conservatism) with regard to seismic actions for the CW and the IS. Other criteria related to the control of the radioactive leakage did govern in the original design. Also, the fragility curves (Figs. 14a and b) are the graphical presentation of Eq. (3) (Section 6.1) expressed function of the logarithmic standard deviations (randomness) and (uncertainty) for 5%, 50% and 95% of the no-exceedance probability, *Q*. On the other hand, as shown by Fig. 14c, the safety goals are respected for this plant. In fact, the capacity in terms of HCLPF is higher for both IS and CW than the acceptance criteria limits for SCDF (0.38 g) and LRF (0.8 g).

7. Conclusions

This paper, presents an original procedure for generating FRS for a CANDU 6 reactor building in operation with a particular attention for the requirement to be used for the equipment assessment. To this end, a special attention is given to adequately represent the dynamic response to seismic records. Hence, a 3D FEM is used instead of a stick model, and the numerical model is calibrated with ambient vibrations measurements results instead of using nominal dynamic material properties. The calibrated 3D FEM is then used for generating FRS based on ground motion time histories compatible with the UHS.

Furthermore, the seismic wave incoherency effect is considered to reduce the ground motion intensity and filter out the high frequency content, mainly from 10 Hz and above, using the ITF method which can be easily implemented in commercial software. It is well demonstrated that the consideration of the beneficial effect of the wave incoherency for the reactor building leads to a reduced seismic demand and, therefore, to a realistic design of equipment sensitive to high-frequency content, namely for 10 Hz and above.

Moreover, the methodology adopted for the seismic fragility analyses of a CANDU 6 reactor building is presented. The fragility analyses are mainly based on the Electric Power Research Institute (EPRI) approach combined with structural models calibrated with ambient vibrations measurements results to reduce both epistemic and aleatory uncertainties. The results are presented for the containment wall and for the internal structure.

Within the PSA, theses seismic fragility analyses are an important step in the evaluation of the seismic margins with regard to the capacity of components (structures) of the plant to sustain the new seismic demand.

References

Abrahamson, N.A., Bommer, J., 2005. Probability and uncertainty in seismic hazard analysis. Earthquake Spectra 21 (2), 603–607.

Adams, J., 2015. New and updated seismic provisions of the 2015 national building code (NBC) of Canada. In: Proceedings of the 11th Canadian Conference on Earthquake Engineering, July 21–24, Victoria, BC, Canada.

AECL, 1974. Design guide addendum, floor response spectra analysis for Gentilly 2 reactor building. DG-66-01092-1.

ASCE 4-98, 2000. Seismic Analysis of Safety-Related Nuclear Structures and Commentary.

ASCE/SEI 43-05, 2005. Seismic Design Criteria for Structures, Systems, and Components in Nuclear Facilities.

Ake, J., Pires, J., Munson, C., 2015. Current and future application of seismic research activities at the NRC in response to the accident at the Fukushima Daiichi nuclear power plant. IAEA-IEM8, Feb 15, 2015 (available on web).

Atkinson, G.M., Pierre, J.R., 2004. Ground-motion response spectra in eastern North America for different critical damping values. Seismol. Res. Lett. 75, 541–545.

CANATOM, 1973. Drawings 1666-21060-101-01-DGAE and 1666-21060-102-01-DGAE. Reactor Building, Loads.

Choi, I.K., Choun, Y.S., Ahn, S.M., Seo, J.M., 2008. Probabilistic seismic risk analysis of CANDU containment structure for near-fault earthquakes. Nucl. Eng. Des. 238, 1382–1391.

Choi, S., Park, S., Hyun, C.H., Kim, M.S., Choi, K.R., 2010. Modal parameter identification of a containment using ambient vibration measurements. Nucl. Eng. Des. 240, 453–460.

Choi, S., Park, S., Hyun, C.-H., Kim, M.-S., 2013. In operation modal analysis of containments using ambient vibration. Nucl. Eng. Des. 260, 16–29.

CSA-N289.1, 2008. General Requirements for Seismic Design and Qualification of CANDU Nuclear Power Plants.

CSA-N289.2, 2010. Ground Motion Determination for Seismic Qualification of Nuclear Power Plants.

CSA-N289.3, 2010. Design Procedures for Seismic Qualification of CANDU Nuclear Power Plants.

DS Simulia, 2008. ABAQUS Version 6.8, User Manual.

El Khoraibi, T., Hashemi, A., Ostadan, F., 2014. Probabilistic and deterministic soil structure interaction analysis including ground motion incoherency effects. Nucl. Eng. Des. 269, 250–255.

EPRI (Electric Power Research Institute), 1991. A methodology for assessment of nuclear power plant seismic margin, EPRI NP-6041-SL, revision 1, project 2722–23, final report.

EPRI, 1994. A Methodology for Developing Seismic Fragilities, EPRI TR-103959 Research Project, Final Report.

EPRI, 2002. Seismic fragility application guide, EPRI 1002988, final report.

EPRI, 2005. Effect of Seismic Wave Incoherence on Foundation and Building Response. Program on Technology Innovation: 1012966.

EPRI, 2006. Effect of Seismic Wave Incoherence on Foundation and Building Response. Program on Technology Innovation: 1013504.

EPRI, 2007. Validation of CLASSI and SASSI Codes to Treat Seismic Wave Incoherence in Soil-Structure Interaction (SSI) Analysis of Nuclear Power Plant Structures. Program on Technology Innovation: 1015111.

Hydro-Québec, 2009a. Earthquake Hazard Analysis: Gentilly Site, Hydro-Quebec Updated seismic hazard estimates (UHS 2008). Prepared by G.M. Atkinson.

Hydro-Québec, 2009b. Time histories for Gentilly 1/10,000 p.a. UHS. Prepared by G. M. Atkinson.

Hydro-Québec, 2010a. Design Guide, Seismic requirements and methodology for Gentilly-2 life extension, prepared by AECL.

Hydro-Québec, 2010b. Seismic fragility analysis of structures, reactor building of Gentilly 2 nuclear power plant, prepared by A. Nour and A. Cherfaoui.

IAEA INSAG-12, 1999. Basic Safety Principles for Nuclear Power Plants, 75-INSAG-3, Revision 1, October.

IAEA, 2004. Geotechnical Aspects of Site Evaluation and Foundations for Nuclear Power Plants. NS-G-3.6 safety guide of the International Atomic Energy Agency.

IZIIS, 2008. Experimental in-situ testing of NPP Gentilly-2 by ambient vibration method. Report prepared for Hydro-Québec.

Kennedy, R.P., Cornell, C.A., Campbell, R.D., Kaplan, S., Perla, H.F., 1980. Probabilistic seismic safety study of an existing nuclear power plant. Nucl. Eng. Des. 59, 315–338.

Lamarche, C.P., 2008. Modal Identification from Ambient Responses of the Gentilly II Nuclear Power Plant. Validation report prepared for Hydro-Québec.

Lee, N.H., Song, K.B., 1999. Seismic capability evaluation of the prestressed/reinforced concrete containment, Yonggwang nuclear power plant, Units 5 and 6. Nucl. Eng. Des. 192, 189–203.

Mandal, T.K., Ghosh, S., Pujari, N.N., 2016. Seismic fragility analysis of a typical Indian PHWR containment: comparison of fragility models. Struct. Saf. 58, 11–19.

Muta, H., Muramatsu, K., Furuya, O., Uchiyama, T., Nishida, A., Takada, T., 2016. Development of a new mathematical framework for seismic probabilistic risk assessment for nuclear power plants – plan and current status – In: Kamae K., (Ed.), Chapter 11 in the book Earthquakes, Tsunamis and Nuclear Risks, Springer.

McGuire, R.K., Cornell, C.A., Toro, G.R., 2005. The case for using mean seismic hazard. Earthquake Spectra 21 (3), 879–886.

Kinemetrics Inc., 2007. High Dynamic Range, IP Aware, Communication Centric Multi-channel Accelerograph or Recorder, Pasadena, CA, USA.

NBCC, 2010. National building code of Canada.

NBCC, 2015. National building code of Canada.

NEA/CSNI/R-9, 2015. Current Practices in Defining Seismic Input for Nuclear Facilities.

NUREG-1407, 1991. Procedural and Submittal Guidance for Individual Plant Examination for External Events (IPEEE) for Severe Accident Vulnerabilities, US NRC, June, KIN 07.

Park, Y.J., Hofmayer, C.H., Chokshi, N.C., 1998. Survey of Seismic fragilities used in PRA studies of nuclear power plants. Reliability Eng. Syst. Saf. 62 (3), 185–195.

RD-152, 2009. Canadian Nuclear Safety Commission Draft Regulatory Document. Guidance on the Use of Deterministic and Probabilistic Criteria in Decision-making for Class I Nuclear Facilities, September.

S-294, 2005. Regulatory Standard. Probabilistic Safety Assessment (PSA) for Nuclear Power Plants, CNSC, April.

Tuttle, M., 2008. Paleoseismic Investigation of Long-Term Rates of Large Earthquakes in the Charlevoix Seismic zone and Proposed Rabaska Site Region. Report to Rabaska, Montreal, Quebec.

Varpasuo, P., 1999. The development of the floor response spectra using large 3D model. Nucl. Eng. Des. 192, 229–241.